

Singularity Formation in 2+1 Wave Maps

James Isenberg

*Department of Mathematics
University of Oregon, Eugene, OR 97403*

Steven L. Liebling

*Theoretical and Computational Studies Group
Southampton College, Long Island University, Southampton, NY 11968*

We present numerical evidence that singularities form in finite time during the evolution of 2+1 wave maps from spherically equivariant initial data of sufficient energy.

98.80.-k, 11.10.Lm, 11.27.+d

I. INTRODUCTION

While it has been shown that wave maps on a 1 + 1 dimensional Minkowski spacetime base evolved from smooth initial data exist for all time [1,2], and that those on an $m + 1$ ($m \geq 3$) Minkowski spacetime base can blow up in finite time [3], global existence for the 2 + 1 case remains as yet unresolved. Scaling considerations identify 2+1 as the critical dimension for wave maps, and so there is considerable interest in determining if indeed 2 + 1 wave maps developed from smooth initial data can become singular in finite time or not. Here, we describe numerical work which strongly supports the contention that, at least for some sets of smooth initial data, they can.

There are special classes of 2 + 1 wave maps for which global existence has been shown to hold: a) spherically equivariant wave maps with convex [4], or slightly more general targets [5], b) spherically symmetric wave maps with compact targets (plus a further technical condition on the target) [6], c) general wave maps (general target) with sufficiently small energy.

Not included in any of these three classes are spherically equivariant wave maps from 2 + 1 Minkowski spacetime into the round two-sphere with initial data of arbitrary energy. Shatah and Struwe [7] have conjectured that singular behavior should be found in this class. Our numerical results reported here strongly support the validity of this conjecture.

We examine one-parameter families of data, with small values of the parameter corresponding to small energy data and therefore global existence, and with large values of the parameter corresponding to data possibly leading to singularity formation. One might hope to find especially interesting wave map development for data at or near the transition between small and large values. While this sort of “critical” behavior has been seen and studied in 3 + 1 wave maps [8,9], we have not found nearly as clear an indication of universal critical behavior for the present 2 + 1 case. This criticality issue needs further study, and is not treated in this paper. Here, our focus

is on numerical evidence for singular wave map evolution from regular initial data.

We note that our studies of singularity formation in 2 + 1 wave maps have been carried out independently of the work of Bizoń, Chmaj, and Tabor [10] using numerical algorithms which differ from theirs. However their results and ours agree substantially.

II. THE EQUATIONS

Generally a wave map is defined to be a map ϕ^A from a spacetime (the “base”) into a Riemannian geometry (the “target”), with ϕ^A a critical point for the action

$$S[\phi] = \int_{M^{m+1}} \eta^{\mu\nu} g_{AB}(\phi) (\partial_\mu \phi^A \partial_\nu \phi^B) \quad (1)$$

where g_{AB} is the Riemannian metric on the target manifold N^n , and $\eta^{\mu\nu}$ is the (inverse) Lorentz-signature metric on the spacetime M^{m+1} . The Euler-Lagrange equations for this action take the form

$$\partial^\mu \partial_\mu \phi^A + \Gamma_{BC}^A \partial_\mu \phi^B \partial^\mu \phi^C = 0 \quad (2)$$

where Γ_{BC}^A represents the Christoffel symbols corresponding to the target metric g_{AB} . This is a semilinear hyperbolic PDE system for ϕ^A . We note that for certain targets, wave maps are known to physicists as “nonlinear sigma models.”

As noted above, the case of primary interest here is 2 + 1 Minkowski spacetime for the base and the round two sphere for the target. In this case, the wave map PDE system (2) may be rewritten in the following form

$$\square \phi^a + (\partial_\mu \phi^b \partial^\mu \phi^c) \delta_{bc} \phi^a = 0. \quad (3)$$

where the indices a, b, c take the values $\{1, 2, 3\}$ (indexing the ambient Euclidean 3-space for the target two sphere), and δ_{bc} is the metric for this ambient space. If we now impose the condition that the maps ϕ^a be spherically equivariant with angular wrapping number k , and write $\phi^a(r, \theta, t)$ in the “hedgehog” form

$$\phi^a = \begin{pmatrix} \sin \chi(r, t) \sin k\theta \\ \sin \chi(r, t) \cos k\theta \\ \cos \chi(r, t) \end{pmatrix} \quad (4)$$

where r is the radial distance from the origin and θ is the azimuthal angle, then the wave map PDE system (2) reduces to the single equation

$$\ddot{\chi} = \frac{1}{r} (r\chi')' - \frac{k^2 \sin 2\chi}{2r^2} \quad (5)$$

where a prime and a dot denote partial derivatives with respect to r and t respectively. Thus the study of the Cauchy problem for $2 + 1$ spherically equivariant (k -wrapped) wave maps into the round two sphere focuses on finding solutions $\chi(r, t)$ to Eq. (5) with regular initial data $\chi(r, 0)$, $\dot{\chi}(r, 0)$. Note that regularity at $r = 0$ requires that we set $\chi(0, t) = 0$ for all t .

While it may be interesting to examine if there is any variation of the behavior of solutions for wrapping numbers k greater than one, we restrict our attention here to the single angular wrapping case $k = 1$.

As for any field theory on Minkowski space, there is a divergence-free stress-energy tensor $T_{\mu\nu}$ associated with wave maps. From $T_{\mu\nu}$, we obtain the energy density function for spherically equivariant wave maps

$$\rho(r, t) = \frac{1}{2} \left[\dot{\chi}^2 + (\chi')^2 \right] + \frac{\sin^2 \chi}{2r^2} \quad (6)$$

whose integral

$$E(t) = \int_r \rho(r, t) r dr \quad (7)$$

is conserved (ie, $E(t) = E(0)$ for all t). The energy is a useful monitor of numerical accuracy, as discussed below.

III. NUMERICAL STUDIES OF SINGULARITY FORMATION

Our numerical experiments consist of specifying parametrized families of initial data $\{\chi_\lambda(r, 0), \dot{\chi}_\lambda(r, 0)\}$ and numerically evolving a number of sets of such data in each family. A typical family—one of the simplest—is the approximately ingoing Gaussian pulse

$$\begin{aligned} \chi(r, 0) &= Ae^{-(r-R_0)^2/\delta^2} \\ \dot{\chi}(r, 0) &= \chi'(r, 0). \end{aligned} \quad (8)$$

This family has three parameters A , R_0 , and δ , with the most important one for our discussion being the scale parameter A . Note that the ingoing character of these solutions, which results from the choice of $\dot{\chi}(r, 0)$, minimizes outer boundary effects. Note also that while, analytically, $\chi(0, 0)$ is not zero, for the choices of R_0 and δ which we make, we can force $\chi(0, 0)$ to be zero and retain smoothness to within numerical accuracy.

We evolve using a second order finite difference approximation to Eq. (5). We use an iterative Crank-Nicholson scheme implemented with RNPL [11], and also make use of the adaptive mesh framework developed by Chop-tuik [12]. We have verified that the code generates solutions which converge quadratically in the grid spacing and conserve energy. In arguing that we are indeed generating singularities, we will discuss the convergence and energy conservation tests in more detail below.

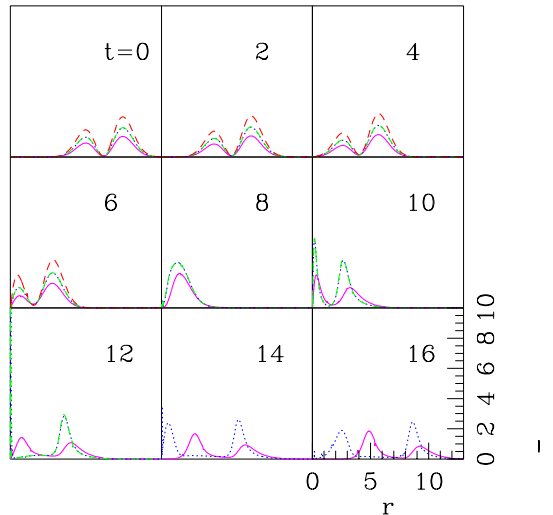


FIG. 1. Snapshots of the energy densities (times r) for a single family of initial data with varying amplitude. At $t = 0$ the initial energy densities corresponding to ingoing Gaussian initial data ($R_0 = 8$, $\delta = 2.3$) are shown. Supercritical ($A = 1.4$) is shown long-dashed (red) which exists only until $t = 6$. Sub-critical ($A = 1.0$) is shown solid (magenta). Two near-critical evolutions are also shown: slightly subcritical ($A = 1.19$) shown dotted (blue) and slightly supercritical ($A = 1.195$) shown short-dashed (green). The two near-critical evolutions coincide at the scale of this graph until $t = 12$ after which we cannot compute the apparently singular supercritical solution. The energy densities reached by the supercritical solutions extend significantly off the scale of this graph.

For a general set of ingoing Gaussian pulse data, regardless of amplitude, the wave map evolution has the pulse maximum and energy density maximum initially moving inward (decreasing r). For small (subcritical) values of A , this inward motion of the maximum proceeds for a finite time, after which the maximum “bounces” away from the origin and begins to move outward (see Fig. 1). There is a general dispersal of the energy density; and for large t , there is very little energy density remaining near the origin.

For large (supercritical) values of A , the behavior of the evolving wave map is qualitatively the same initially. However, rather than bouncing away from the origin, the

maxima for supercritical data continue to approach the origin (Fig. 1), with the concentration of energy around the origin appearing to grow without bound. As the energy density and the gradient of the function χ grow very large at the origin, the numerical evolution inevitably becomes unable to resolve the gradient, and the solution becomes sufficiently non-smooth to cause the numerical evolution to stop. If this accumulation is indeed a singularity forming, there is no hope for the numerical evolution to resolve it, being itself of finite resolution. The task then is to examine the behavior of the numerical solution up to this point.

Before doing so, we first discuss a couple of standard tests of a numerical solution. We let $\chi(r, t)$ be some solution to the (continuum) partial differential equation (5) and let $\tilde{\chi}_h(r, t)$ be the solution to a discrete form of that equation, for corresponding initial data, on a grid spacing $h \equiv \Delta r$. The hope is that, as the grid spacing Δr gets smaller, the solutions to the discrete equation generated by the evolution code converge to the solutions of the PDE, $\tilde{\chi}_h(r, t) \rightarrow \chi(r, t)$. Because in general the explicit solutions to the PDE are unknown, we instead consider a series of numerical solutions on grids of increasing resolution, say $\tilde{\chi}_{4h}, \tilde{\chi}_{2h}, \tilde{\chi}_h$. If these are to converge to the PDE solution, then they must converge themselves. To examine this convergence, we define a convergence factor (Q) as follows

$$Q \equiv \frac{|\tilde{\chi}_{4h} - \tilde{\chi}_{2h}|_2}{|\tilde{\chi}_{2h} - \tilde{\chi}_h|_2}, \quad (9)$$

where the norms are the l_2 norm. For these solutions to converge, the difference between solutions for increasing resolution must decrease and hence Q must be greater than one. For second-order schemes, Q is expected to be 4.

Another common test of numerical accuracy focuses on the degree to which energy is conserved by the numerical evolution. The evolution governed by the PDE (5) does conserve energy; the question is whether this remains true for the numerical evolution. Letting $E_{num}(t)$ denote the energy calculated from the numerical solution at time t (on the finite grid), and setting $\Delta(t) \equiv \ln \left| \frac{E_{num}(t) - E_{num}(0)}{E_{num}(0)} \right|$, we monitor $\Delta(t)$ for different choices of grid spacing. The expectation is that $\Delta(t)$ should decrease with increasing resolution; if we observe this, our confidence in the accuracy of our numerical solution is enhanced.

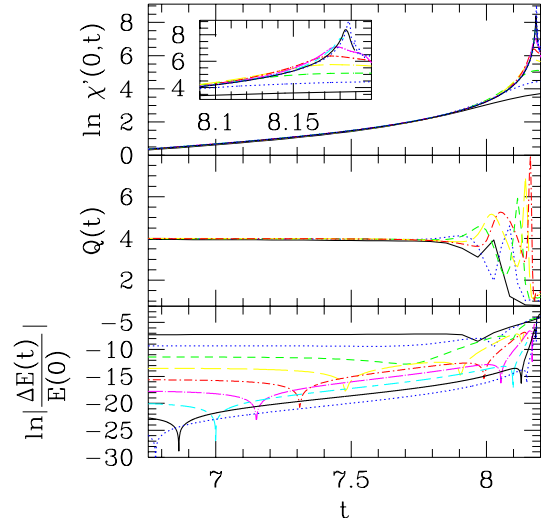


FIG. 2. Results of a super-critical evolution for an initially ingoing Gaussian pulse ($A = 2$, $R_0 = 10$, $\delta = 2.3$, $R_{max} = 30$). The results are shown for increasing resolutions $n = 2^8$ (solid, black), $n = 2^9$ (dot, blue), $n = 2^{10}$ (short dash, green), $n = 2^{11}$ (long dash, yellow), $n = 2^{12}$ (dot-short dash, red), $n = 2^{13}$ (dot-long dash, magenta), $n = 2^{14}$ (short dash-long dash, cyan), $n = 2^{15}$ (solid, black), and $n = 2^{16}$ (dot, blue), where $h = R_{max}/n$. The top frame shows the rapid growth of $\chi'(0, t)$ near the time of the blow-up ($t \approx 8$). The middle frame shows the convergence factor (defined in Eq. (9)). Factors greater than one indicate convergence. The bottom frame shows the change in energy with respect to the initial energy. As the resolution increases, so does the level of energy conservation.

In Fig. 2, we show the evolution in time of three quantities— $\ln \chi'(0, t)$, $Q(t)$, and $\Delta(t)$ —for numerical runs of supercritical ingoing Gaussian pulse data, done with nine different grid spacings. In the top frame, we show the behavior of the derivative of χ at the origin as a function of time. The figure shows that as the pulse travels inward, the derivative increases. Until just before $t = 8$, all the resolutions show the same behavior as would be expected for a convergent evolution. However, near the blow-up time, the solutions diverge with higher resolutions providing a larger derivative. The convergence factor $Q(t)$ is shown in the middle frame; it likewise shows second-order convergence up to times close to the blow-up time. In the bottom frame, the change in energy $\Delta(t)$ is shown. We see that as the resolution is increased, energy conservation improves.

What does this tell us about singularity formulation in wave maps evolved from (supercritical) ingoing Gaussian pulse data? We first argue that these results are consistent with what would be expected for such formation. As the singularity forms, higher and higher frequency components become important, and they are represented numerically only if one uses higher and higher grid res-

olutions. Hence, the behavior of the derivative of χ as the resolution improves would be expected to show larger and larger gradients, as seen in Figure 2a. Next, we note that the formation of a singularity should not hinder convergence except quite near the formation time, as is seen in Figure 2b.. Finally, energy conservation should be fine until the high frequency components play their role, as we see in Figure 2c. Hence, the results observed appear to be consistent with a singularity forming near $t = 8$.

This does not guarantee that a singularity forms in these wave maps. There are other effects that might produce the apparently unbounded growth of the derivative of χ and of the energy density near the origin in these numerical simulations. For example, perhaps some unphysical, unstable mode grows because of the particulars of our chosen evolution scheme. We believe that this is not the case, for a number of reasons. First, the presence of such a mode would likely cause much larger growth in $\Delta(t)$ than we see. Second, such modes would have to be excited only after some time (roughly independent of resolution) and only for families of sufficiently large energy. This is not consistent with our observations. Third, the excitation of this sort of instability would almost certainly depend critically on the precise finite difference scheme. Because Bizoń and his collaborators [10] observe similar behavior, using a different numerical evolution scheme, this does not appear to be the case. Thus we believe it very unlikely that the effects we are seeing are the result of a numerically unstable nonsingular mode.

Another situation in which one might numerically observe the formation of singularities that do not in fact evolve analytically from the corresponding data is if the continuum PDE solution is regularized by high frequency components which cannot be seen by the finite grid resolutions we use. The rather strong convergence behavior we see in our numerical solutions leads us to believe that this is not happening. We note in particular that such unresolved components would have to be separated in frequency space from the nontrivial low frequency components by a substantial margin, with a large range of dynamically irrelevant frequencies separating the two regimes. This seems to be very unlikely.

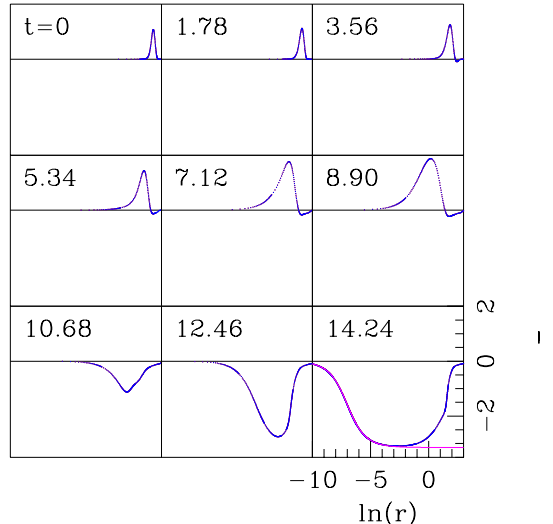


FIG. 3. Near critical evolutions approach the static solution, Eq. (10). Nine frames equally spaced in time are shown for both *sub*- and *super*-critical evolutions. The solutions are indistinguishable in the graph at these times and are shown with dots. After $t = 14.24$, the two solutions have quite different fates, but both approach the form of the static solution. In the final frame, the static solutions $\chi(r) = -2 \arctan(1116r)$ is shown.

IV. CONCLUSION

The numerical studies we present here very strongly support the contention, previously conjectured by Shatah and Struwe [7], that smooth initial data for wave maps from 2+1 Minkowski spacetime into the round two sphere can develop singularities (with unbounded derivatives) in finite time. As we note, there are many ways in which the numerical exploration of possible singularity formation might produce misleading indications. However, we believe that as a consequence of the numerical tests we have carried out, together with those done independently by Bizoń and his collaborators [10], the formation of singularities is the most likely conclusion.

There is much more one would like to know about these spatially equivariant wave maps, as well as about those without such symmetry. One would like to know, for example, if the solutions assume any universal form as one approaches the singularity. Our work (see Fig. 3) supports the results of Bizoń et al [10] which indicate that indeed the family of static spherically equivariant wave maps

$$\chi(r) = \pm 2 \arctan(\lambda r) \quad (10)$$

does serve as a sort of universal model for singularity formation. This needs to be studied further. One would also very much like to understand the behavior of the

wave maps which evolve from initial data near the transition from subcritical to supercritical data. The recent numerical work of Bizoń et al [10] suggests that the static solutions (10) play a central role in the evolution of the transitional wave maps as well in that of supercritical ones; however, this issue needs further investigation. (Note the absence of any self-similar solutions to the 2+1 wave map equations; for 3+1 wave maps, such solutions play a key role in behavior of solutions evolving from critical or near critical data).

ACKNOWLEDGMENTS

We thank Piotr Bizoń for helpful discussions. Partial support for this work has come from NSF Grant PHY-9800732 at the University of Oregon. SLL is appreciative of the support of NSF PHY-9900644 and of the financial support of Southampton College.

- [12] M.W. Choptuik, “Universality and Scaling in Gravitational Collapse of a Massless Scalar Field,” *Phys. Rev. Lett.* **70**, 9-12 (1993).

-
- [1] C. Gu, “On the Cauchy Problem for Harmonic maps Defined on 2 Dimensional Minkowski Space,” *Comm. Pure Appl. Math.* **33**, 727-737 (1980).
- [2] J. Ginibre and G. Velo, “The Global Cauchy Problem for the Nonlinear Klein-Gordon Equations,” *Math. Z.* **180** 487-505 (1985).
- [3] J. Shatah, “Weak Solutions and the Development of singularities in SU(2) Sigma Models,” *Comm. Pure Appl. Math.* **41**, 459-469 (1988).
- [4] J. Shatah, and A.S. Tahvildar-Zadeh, “On the Cauchy Problem for Equivariant Wave Maps,” *Comm. Pure Appl. Math.* **47**, 719-751 (1994).
- [5] M. Grillakis, “Classical Solutions for the Equivariant Wave Map in 1+2 Dimensions,” Preprint.
- [6] D. Christodoulou and A.S. Tahvildar-Zadeh, “On the Regularity of Spherically Symmetric Wave Maps,” *Comm. Pure Appl. Math.* **46**, 1041-1051 (1993).
- [7] J. Shatah and M. Struwe, *Geometric Wave Equations*, Courant Lecture Notes in Mathematics, New York University (1998).
- [8] S.L. Liebling, E.W. Hirschmann, and J. Isenberg. “Critical Phenomena in Nonlinear Sigma Models,” *Journal of Mathematical Physics* **41**, 5691-5700 (2000). math-ph/9911020
- [9] P. Bizoń, T. Chmaj and Z. Tabor, “Dispersion and collapse of wave maps,” *Nonlinearity* **13**, 1411 (2000). math-ph/9912009
- [10] P. Bizoń, T. Chmaj and Z. Tabor, “Formation of singularities for equivariant 2+1 dimensional wave maps into 2-sphere,” LANL preprint: math-ph/0011005 (2000). To be published in *Nonlinearity*
- [11] Software available from <http://laplace.physics.ubc.ca/Members/matt/Rnpl/index.html>